ISSN: 0975 -8542

Journal of Global Pharma Technology

Available Online at: www.jgpt.co.in

RESEARCH ARTICLE

Effect of Functionalized Graphene Oxide (FGO) on the Electrical and Dielectrical Properties of PVA Films

Sundus H. Merza

Department of Chemistry, College of Education for Pure Science /Ibn-Al-Haitham, University of Baghdad, Iraq.

Abstract

In the present work, nanocomposite of poly (vinyl alcohol) (PVA) incorporated with functionalized graphene oxide (FGO) were fabricated using casting method. PVA was dispersed by varying content of FGO (0.3, 0.5, 0.8, 1 wt %). The PVA- FGO nanocomposite was characterized by FT-IR, FE-SEM and XRD. Frequency dependence of real permittivity (ε'), imaginary (ε") and a.c conductivity of PVA/FGO and PVA/GO nanocomposite were studied in the frequency range 100 Hz- 1 MHz. The experimental results showed that the values of real (ε') and imaginary permittivity (ε") increased dramatically by increasing the FGO content in PVA matrix. PVA/ FGO (1 wt %) nanocomposite revealed higher electrical conductivity of 6.4×10^{-4} Sm^{-1} compared to 1.4×10^{-8} Sm^{-1} for PVA/GO

Keywords: *Dielectric spectroscopy, Functionalized Graphene oxide, Nanocomposite, PVA, Maxwell-Wagner-Sillars polarization.*

Introduction

Dielectric spectroscopy can be applied for all non-conducting or semiconducting materials and their interaction can determined with an alternating electric field over wide range of frequencies. Materials with low and high dielectric constant are essential in electronic industries and have very broad applications, including insulators, dielectric amplifiers, semiconductor devices, capacitors, piezoelectric transducers, and memory elements etc [1].

PVA an insulating polymer has excellent film forming and adhesive properties and thus commonly used to fabricate new composite and membrane [2].PVA acquire special attention in fibre and non fiber industry, pharmaceutical, biomedical and biochemical applications [3].Many researchers have reported methods to improve its electrical and dielectrical properties using various doping agent [4, 5].

In particular graphitic nanostructures such as CNT, graphene and graphene oxide are attracted the attention of research community due to their unique mechanical, electrical and optical properties [6, 7]. Few studies have been made to investigate the effects of different functional groups of GO on dielectric properties of PVA [8].

According to the concept, GO functionalized with Triazole ring was successfully fabricated and used as filler to generate new nanocomposite with PVA. The results were reported in terms of the real, imaginary components of the complex permittivity, and ac conductivity. The effects of weight content of functionalize GO (FGO) on the electrical and dielectric behavior of PVA composite was studied.

Experimental Details

Chemicals and Reagents

Ploy (vinyl alcohol) (PVA) fully hydrolyzed has residual acetyl groups from SIGMA. Hydrazine (N_2H_4) and carbon disulfide (CS_2) anhydrous ≥99 from ASPAIN. All other chemicals were analytical grade and purchased from Fluka.

Apparatus

Dielectric properties of nanocomposite PVA/FGO were studied at frequency range of 100Hz-1MHz by using LCR-8101G.

Functionalized GO was dispersed with an Ultrasonic instrument type soniprep 150(United Kingdom). Powder XRD analysis was carried out by using powder diffractometer (Japan) XRD Shimadzu 6000 with an incident Cu-Kα radiation of 1.54A° 40.0Kv and 30mA; scan range (2θ= 5-80°) and; scan speed: 10 (deg/min). FT-IR spectra of films were obtained on Shimadzu IR affinity 8400s, Japan. Scan range of 4000-400 cm^{-1} with an attenuated total reflection accessory. Field-Emission scanning electron microscope FE-SEM model MIRA3- TESCAN French was used to investigate the morphology of nanocomposite.

Preparation of Nanocomposite

Graphene oxide (GO) was synthesized by hummers' method [9]. The GTO mixture formed was filtered and washed by 5% aqueous solution HCL and distilled water until the pH of the rinsing water became (6-7). The product was dried at 55° for 48h. The graphite oxide GTO aqueous solution mixture was exfoliated by sonication [10].The edge-Functionalized graphene oxide (E-FGO) was prepared as previous work [11]. Thiocarbohydrazide TCH was prepared from reaction of hydrazine N_2H_4 with carbon disulfide CS_2 [12]. Desired amount of TCH with GO was heated at 168 c°for 10min. The product FGO was cooled washed with distilled water to dissolve the TCH none reacted and dried at 60c°.

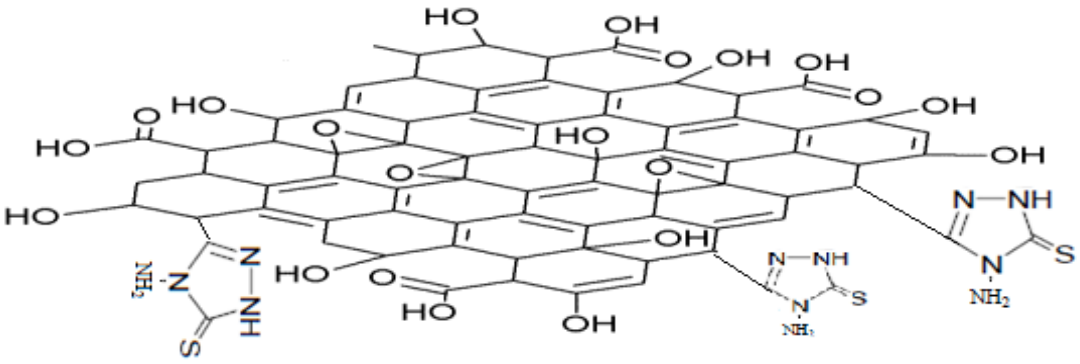

Figure 1: Structure of FGO

The sonicated functionalized GO(FGO) solution was slowly transferred to the 10% PVA solution in quantities that gave 0.3,0.5,0.8 and 1 wt % filler loading on the final films, namely PVA/FGO (0.3), (0.5), (0.8), (1). The solution was stirred for 2 h to avoid any agglomeration and to obtained uniform dispersion. For comparison, a film of PVA/GO was also prepared by the same procedure. Casting of the resulting homogeneous solutions at room temperature in square glass gave the desired PVA/FGO nanocomposite. The films was slowly pulled out and used for characterization.

Result and Discussion

FT-IR spectroscopy was carried out in order to determine the hydrogen bonding interactions between the FGO, GO with PVA matrix, The FT-IR spectra of neat PVA, PVA/GO and PVA/FGO have shown in Figure 2. The spectrum of neat PVA show characteristic absorption peaks at 3284.88 cm^{-1} which can be ascribed to O-H stretching vibration. The bands at 2937 cm^{-1}, 2908.75 cm^{-1} are attributed to asymmetric and symmetric stretching of CH_2.

Furthermore, the bands at 1707.06 and 1716.70cm^{-1} belong to residual acetyl groups remaining in fully hydrolyzed PVA. The band at 1564.32 cm^{-1} due to water absorption, the peaks at 1417.73 cm^{-1}, 923.93 cm^{-1} assigned to CH_2 bending and rocking respectively, the (OH) rocking with CH wagging appeared at 1325.14 cm^{-1} the band appears as shoulder at 1141.90 cm^{-1} refer to crystalline sequence of PVA[13].

The absorption at 1087.89 cm^{-1} and 833.28 cm^{-1} refer to C-O and C-C stretching [14].

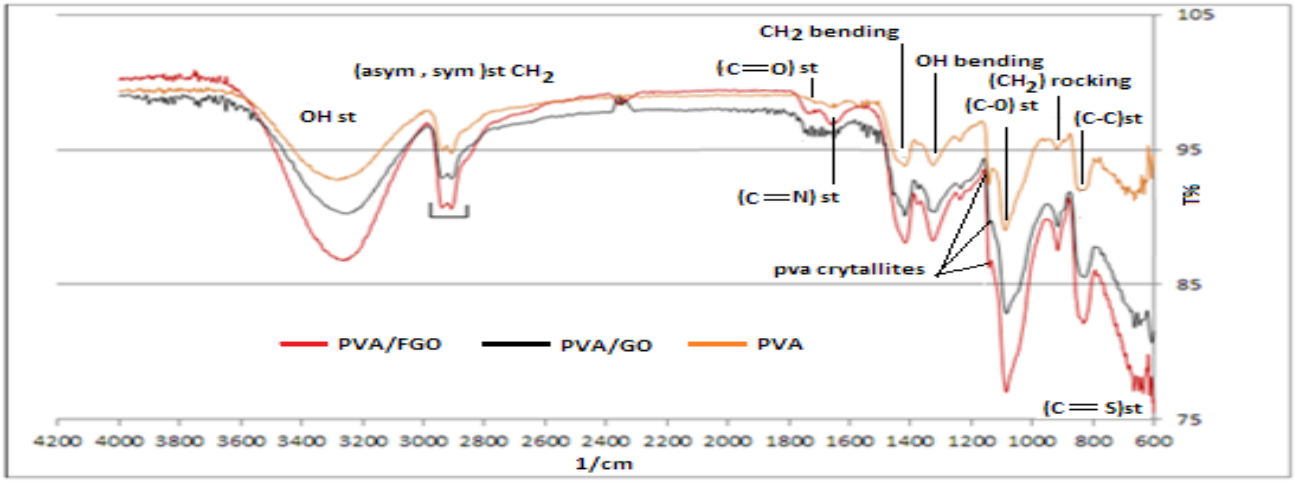

Figure 2: FT-IR spectrum of neat PVA, PVA/GO and PVA/FGO

The absorption bands located at ~670 cm^{-1} and (1600-1700) belong to (C=S) st and (C=N) st respectively of FGO [16]. The increase in the O-H and C-O stretching vibration, can be attributed to the presence of hydrogen bonding interactions between functional groups of GO and FGO with the hydroxyl groups on PVA molecular chains [15]. Compared with neat PVA, the surface of the nanocomposite shows FGO appears as dots having different sizes. In addition, FGO flakes dispersed homogeneously in the PVA matrix indicating that the Triazole rings in FGO improve the compatibility between PVA and FGO. The surface images of the neat PVA and PVA/FGO composite are shown in Figure 3 (A and B respectively).

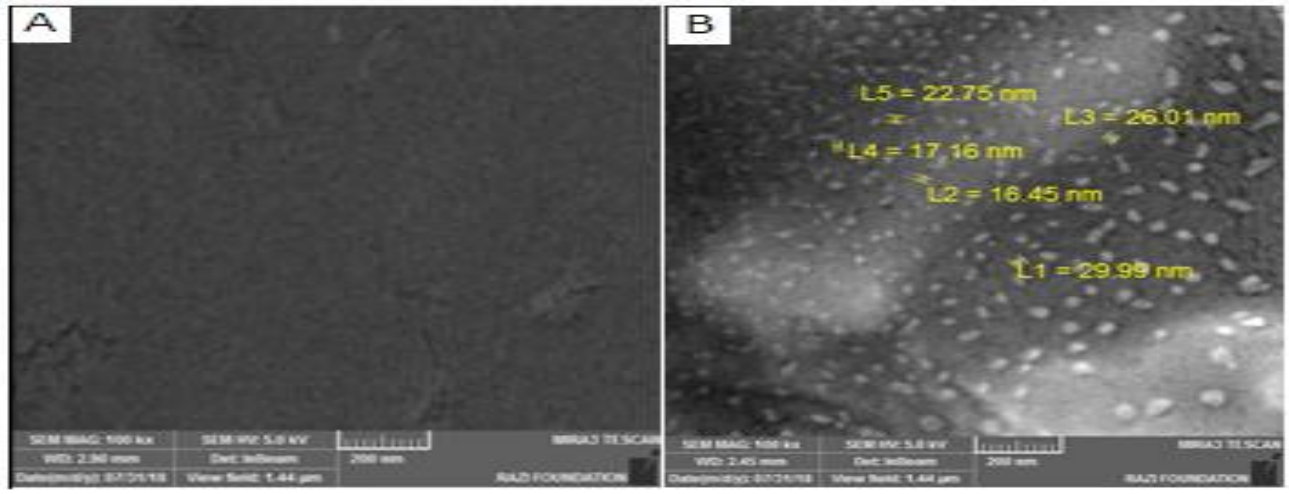

Figure3: FE-SEM image of neat PVA (A) and PVA/FGO (B) with 200nm magnification

The XRD pattern of the prepared FGO exhibits an emergence a new well-defined Bragg reflections at 2θ angles due to the edge functionalities, Figure 4.

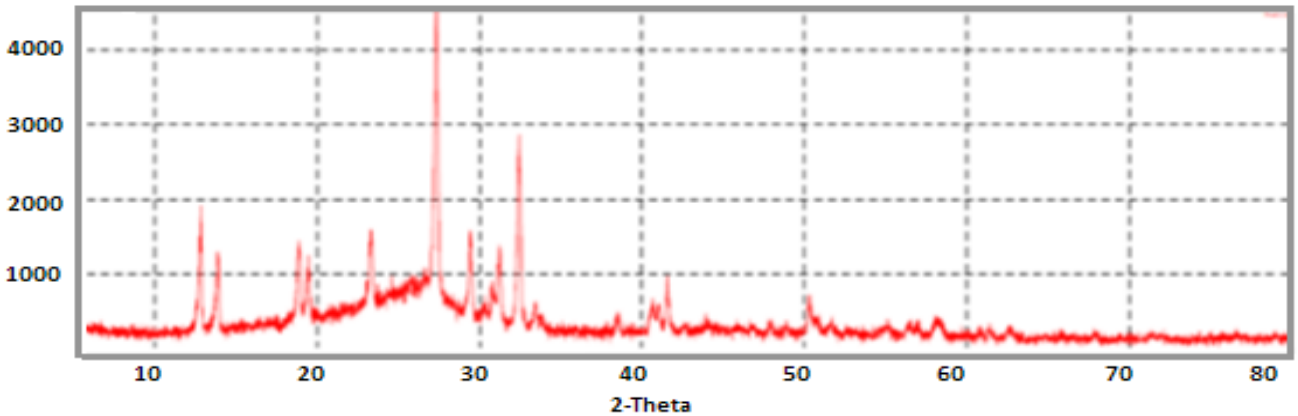

Figure 4: XRD pattern of FGO

Figure (5) shows the XRD patterns for neat PVA, 0.3 wt %, 0.5 wt %, 0.8 wt % and 1 wt % PVA/FGO composite. As indicated in this Figure, neat PVA has only one peak at around 2θ = 19.6° (d =4.50 A) belong to Semicrystalline reflections of PVA consistent with previous reports [17, 18].

The characteristic peaks of FGO cannot be detected in the XRD pattern of PVA/FGO, suggesting that FGO nanosheets can uniformly disperse in PVA. The broad amorphous band that appeared at high content of FGO may be belong to stacked FGO nanosheets.

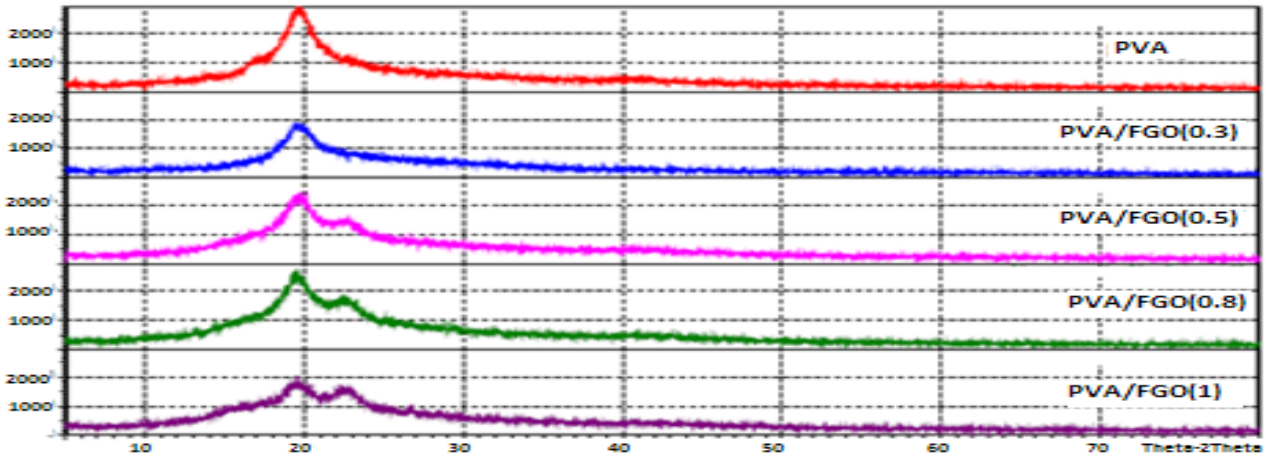

Figure 5: X-ray diffraction of neat PVA and nanocomposite with different content of FGO

The dielectric performance of the neat PVA, PVA/FGO and PVA/GO dielectric film was measured at frequencies in the range of 100 Hz to 1 MHz. The real permittivity (ε') of nanocomposite with different weight loading was measured aided by the following expression: [19].

$$\varepsilon' = c\, d/\varepsilon^{\circ}\, \mathrm{A}$$

Where (ε°), (d), and (A) are the permittivity of free space (8.854×10^{-12}) F.m^{-1}, thickness of the sample and the area of the electrode (m^2) respectively. The frequency dependence of real permittivity (ε') of PVA/FGO nanocomposite films at $25^{\circ}C$ is shown in Figure 6. The dielectric constant of PVA/FGO (1wt%) nanocomposite film compared with PVA/GO (1)wt% the inset Figure is ten order in magnitude due to contribution of molecular dipoles of the functional groups(amine outside the plane) attached at the edge of GO flake and may attributed to the good compatibility between phases.

As the content of functionalities decrease and loading less than (0.8) wt% the real permittivity shows weak frequency dependence. At low frequencies, the real permittivity of PVA/ FGO (0.8wt%) and (1wt%) films have higher value due to that the molecular dipoles have sufficient time to align themselves according to the applied field , where as its values decreased slowly at the higher frequencies region because they could not follow the field oscillating [20].

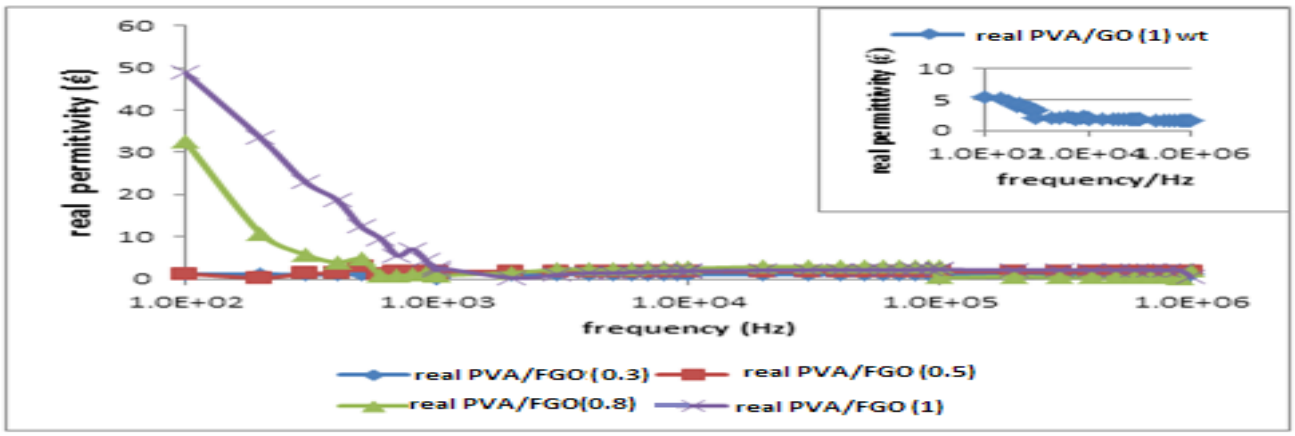

Figure 6: Frequency dependences of the real permittivity (ε') for the PVA/FGO composites with different FGO contents (0.3), (0.5), (0.8) and (1) wt %.(inset) of PVA/GO (1) wt%

The frequency dependence of imaginary part of the complex permittivity of the PVA/FGO composites at 25°C is shown in Figure 7. The imaginary permittivity is substantially increased significantly when The FGO concentration is above 0.5 wt% due to increases the concentration of the mobile charges in the composites. When the frequency is higher than 10 KHz, the imaginary permittivity decreases and show weak frequency dependence. The insets Figure refer to imaginary permittivity of PVA/GO.

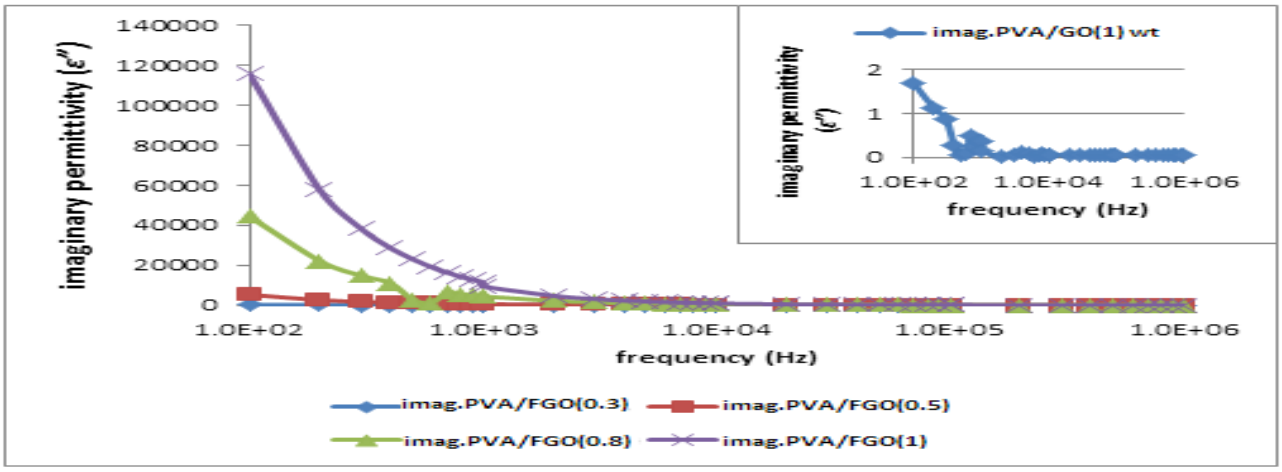

Figure 7: Frequency dependences of the imaginary permittivity (ε") for the PVA/FGO composites with different FGO contents of (0.3), (0.5), (0.8),and (1) wt%

The jump in the real and imaginary permittivity values at (0.5) wt% FGO [figure (8)] confirming that the composite transition to conducting percolation region and it can able to build network that facilitates electron hopping or tunneling.

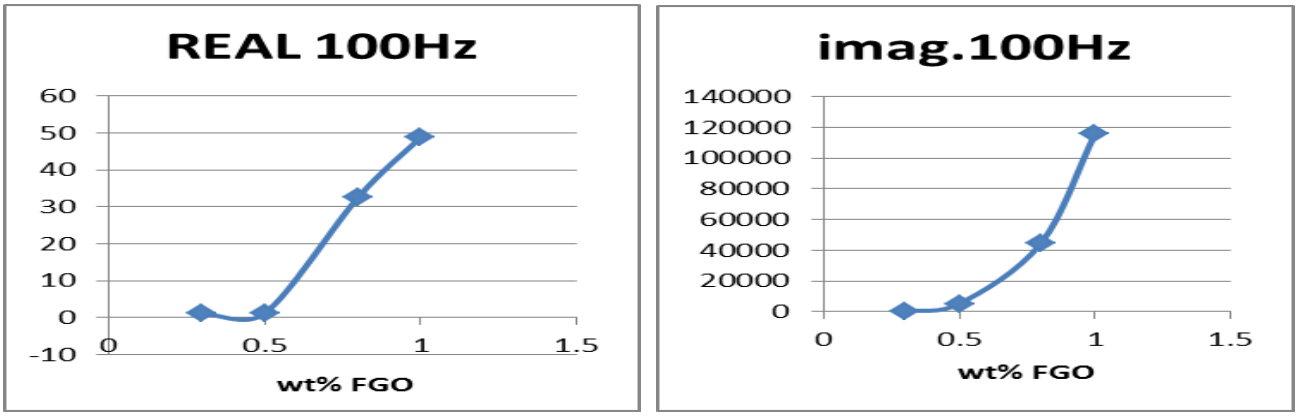

Figure 8: real and imaginary permittivity of PVA/FGO versus weight content of FGO at 100Hz

The dielectric loss is a material property which is a measure of energy loss in the dielectric material during AC measurement .loss tangent (tan δ) or the dissipation factor (D) are synonymous of the dielectric loss define as the ratio of the imaginary part of the permittivity to the real part of the permittivity as shown in the following equation [21, 22].

$\tan\delta = \varepsilon'' / \varepsilon'$ (3-4)

Experimentally Table 1 represents the dielectric loss (D) that are measured for prepared nanocomposite PVA/GO and PVA/FGO at selected frequencies (100Hz, 100KHz, and 1MHz) respectively. It can be seen from this table that the (D) of PVA/FGO increased by increasing weight fraction of FGO doping, increasing the dissipation factor may be due to the existence of a strong polarized interface or Maxwell-Wagner-Sillars polarization. This mechanism occurs at the interface between materials with different permittivities and/or conductivities due to the accumulation of virtual charges at the filler/polymer interface [23, 24] PVA/GO has lower dissipation factor values.

Table 1: Dielectric loss (D) that are measured for prepared nanocomposite PVA/GO and PVA/FGO at selected frequencies

Content wt%	Dissipation factor At 100Hz		Dissipation factor At 100KHz		Dissipation factor At 1MHz	
	PVA/GO	PVA/FGO	PVA/GO	PVA/FGO	PVA/GO	PVA/FGO
0.3	0.0877	163.7	0.0345	0.28	0.0548	0.0603
0.5	0.0932	4337	0.0249	0.2855	0.0269	0.2394
0.8	0.193	1362	0.0303	1.532	0.0393	0.6008
1	0.6119	2371	0.0302	4.0749	0.0380	4.3453

The a. c conductivity (S.m^{-1}) of PVA/FGO and PVA/GO nanocomposite films was calculated by the relation below [25].

$\sigma_{a.c}=\omega\varepsilon^{\circ}$ è $tan\delta$ (3-6)

Where ω was the angular frequency which equals to (2πf).Figure (9) represents the a.c conductivity of the nanocomposite as a function of frequencies for different weight percent of PVA/FGO films. The a.c conductivity of PVA/FGO nanocomposite increased dramatically upon increasing the FGO concentration. FGO (1wt%) increased about four orders of magnitude upon PVA/GO, this may be that FGO served at this critical concentration as a conducting bridge to link PVA. also the a.c conductivity decreased gradually by increasing applied field frequency.

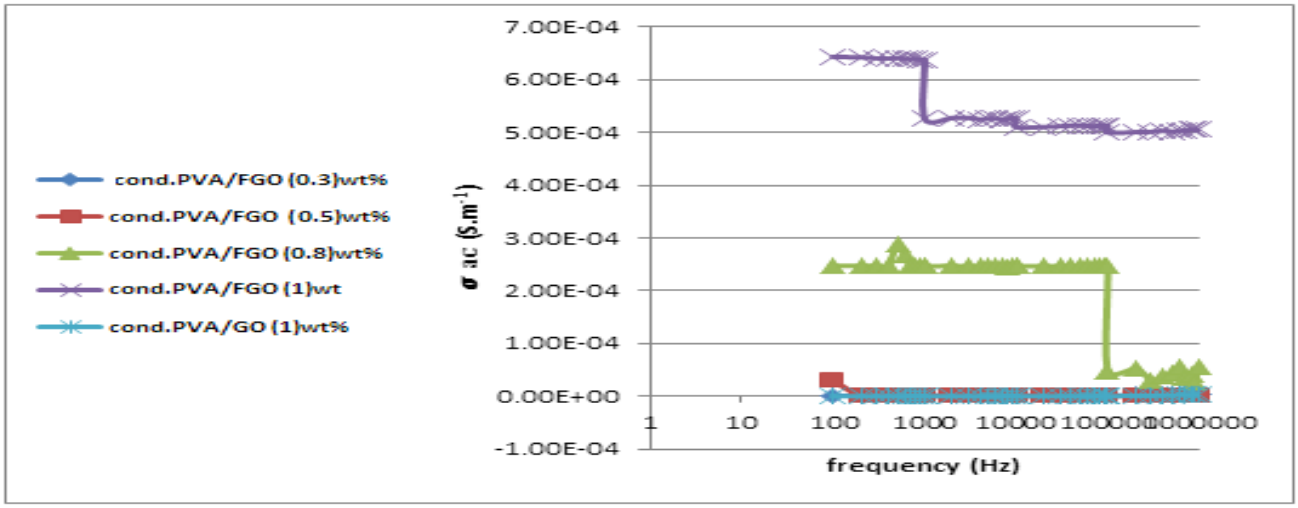

Figure 9: Frequency dependences of the a.c conductivity for the PVA/FGO nanocomposite with different FGO contents of FGO (0.3), FGO (0.5), FGO (0.8), FGO (1)

Conclusion

In this study, PVA-based nanocomposite filled with FGO was prepared by solvent casting route and characterized .FTIR and XRD analysis of the PVA/FGO nanocomposite suggested that the addition of FGO in PVA matrix enhance interactions within the composite due to increasing functional groups. It has been observed that the concentration FGO has greatly influenced the dielectric properties of PVA matrix. As FGO content increase, the real and imaginary parts of dielectric constant increased dramatically due to orientation of the polar group. Electrical conductivity of the nanocomposite was obtained by the LCR spectroscopy and increased gradually by increase the amount of FGO and was not affected by the addition of low FGO concentrations.

References

1. Polymer Nanocomposites (2016) Electrical and Thermal Properties, Huang, Xingyi, Zhi, Chunyi, Switzerland, Springer.
2. WY Chuang, TH Young, WY Chiu, CY Lin (2000) Polymer, 41: 5633-5641.
3. C Shao, HY Kim, J Gong (2003) Materials Letters, 57: 1579.
4. Y Bao, JW Zha, J Zhao, ZM Dang, GH Hu (2012) ACS Appl. Mater. Interfaces, 4: 6273-6279.
5. M Şimşek, ZMO Rzayev, S Acar, B Salamov, U Bunyatova (2016) SPE.
6. D Cai, M Song (2010) Journal of Materials Chemistry, 20: 7906-7915.

7. Z Spitalsky, D Tasis, K Papagelis, C Galiotis (2010) Progress in Polymer Science, 35: 357-401.
8. X Zheng, H Yu, Sh Yue, R Xing, Q Zhang1, Y Liu, B Zhang (2018) Int. J. Electrochem. Sci., 13: 1-13.
9. WS Hummers, RE Offeman (1958) Journal of the American Chemical Society, 80(6): 1339-133.
10. I Jung (2007) Nano Lett., 7: 3569-3575.
11. IA Latif, SH Merza (2018) Abn Al-Haitham Jour. for Pure & Appl. Sci., 31: 1.
12. S XH, LY Burn (1999) China 621: 46-48.
13. B Hamouda, S Nguyen, QT Langevin, D Roudesli (2010) CR Chim, 13: 372-379.
14. AS Asran, S Henning, GH Michler (2010) Polymer, 51: 868-876.
15. IM Jipa, A Stoica, M Stroescu, LM Dobre, T Dobre, S Jinga, Ch Tardei (2012) Chemical Papers, 66 (2): 138-143.
16. OV Smirnova, AG Grebenyuk, GI Nazarchuk, Yu L Zub (2015) Chemistry, Physics and Technology of Surface, 6(2): 224-23.
17. GK Prajapati, PN Gupta (2011) Physica B: Condensed Matter, 406: 3108-3113.
18. YM Lee, SH Kim, SJ Kim (1996) Blend Polymer, 37: 5897.
19. MH Harun, E Saion, A Kassim, E Mahmud, MY Hussain, IS Mustafa (2009) J. Adv. Sci. Arts, 1: 9-16.
20. V Raja, AK Sharma, N Rao (2004) Materials Letters, 58: 3242-3247.
21. Fundamentals of ceramics. International Editions, W.B. Michel, McGraw-Hill companies, Inc. New York, 371(1997).
22. Physics of dielectric Materials, B Tarrev (1979) Mir publishes Moscow, translated from the Russian.
23. M Molberg, D Crespy, P Rupper, F Nuesch, J Manson, C Lowe, DM Opris (2010) Advanced Functional Materials, 20: 3280-3291.
24. H Stoyanov, M Kollosche, S Risse, D McCarthy, G Kofod (2011) Soft Matter, 7: 194-202.
25. GK Raheem, MA Habeeb, QM Jebur (2017) Journal of Chemical and Pharmaceutical Sciences, 10: 1.